Research Article

For reprint orders, please contact: reprints@futuremedicine.com

Future MICROBIOLOGY

Green synthesis of silver nanoparticles combined to calcium glycerophosphate: antimicrobial and antibiofilm activities

José AS Souza[1], Debora B Barbosa[2], Andresa A Berretta[3], Jackeline G do Amaral[1], Luiz F Gorup[4], Francisco N de Souza Neto[4], Renan A Fernandes[2], Gabriela L Fernandes[2], Emerson R Camargo[4], Alessandra M Agostinho[5] & Alberto CB Delbem*,[1]

[1]Department of Pediatric Dentistry & Public Health, São Paulo State University (UNESP), School of Dentistry, Araçatuba, São Paulo, 16015-050, Brazil

[2]Department of Dental Materials & Prosthodontics, São Paulo State University (UNESP), School of Dentistry, Araçatuba, São Paulo, 16015-050, Brazil

[3]Laboratory of Research, Development & Innovation, APIS FLORA INDL. COML. LTDA., Ribeirão Preto, São Paulo, 14020-670, Brazil

[4]Department of Chemistry, Federal University of São Carlos, São Carlos, São Paulo, 13565-905, Brazil

[5]Department of Microbiology & Molecular Genetics, Michigan State University, East Lansing, 48824 MI, USA

* Author for correspondence: Tel.: +55 18 3636 3314; Fax: +55 18 3636 3332; adelbem@foa.unesp.br

Aim: To synthesize, characterize and evaluate the antimicrobial and antibiofilm activities of novel nanocomposites containing silver nanoparticles (AgNPs) associated or not to β-calcium glycerophosphate. **Materials & methods:** These nanocomposites were produced through a 'green' route using extracts of different parts of pomegranate. Antimicrobial and antibiofilm properties against *Candida albicans* and *Streptococcus mutans* were determined by the minimum bactericidal/fungicidal concentration and biofilm density after treatments. **Results:** All extracts used were successful in producing AgNPs. Composites made with peel extracts showed the highest antimicrobial and antibiofilm activity against both microorganisms tested and performed similarly or even better than chlorhexidine. **Conclusion:** AgNPs associated or not to calcium glycerophosphate produced by a 'green' process may be a promising novel antimicrobial agent against oral microorganisms.

First draft submitted: 10 August 2017; Accepted for publication: 17 October 2017; Published online: 14 February 2018

Keywords: biofilm • 'green' synthesis • silver nanoparticles

Biofilms are defined as microbial communities that can harbor multiple bacterial and fungal species [1], embedded in an extracellular polymeric substances and are associated to virtually any surface on the planet including hard and soft tissues of humans [2]. In the oral cavity, in particular, the accumulation of acidogenic biofilms on tooth surfaces causes the dissolution of the enamel, a process known as demineralization [3], which if maintained for prolonged periods may lead to development of dental caries.

One of the main etiological agents in caries is *Streptococcus mutans* [4], a Gram-positive, facultative anaerobic, coccus-shaped bacterium, which is able to ferment several sugars, including sucrose, glucose, dextrose and lactose, producing lactic acid [5]. But recently, studies have demonstrated a significant association between *S. mutans* and *Candida albicans* and early childhood caries [6,7]. *C. albicans* is a commensal fungal species commonly colonizing human mucosal surfaces and, as *S. mutans*, presents high acidogenic and cariogenic potentials [8]. In 97% of children with caries, *C. albicans* can be isolated from dental lesions [9]. In fact, many *in vitro* studies have shown that *C. albicans* can enhance the adherence of *S. mutans* indicating a possible mechanism of interaction between them [10].

Controlling oral biofilm formation is not an easy task but in recent years, nanotherapeutics have been used with success by incorporating nanoparticles into several dental materials [11,12]. Silver nanoparticles (AgNPs) have gained importance in medicine, biology, physics and chemistry fields [13–15] due to antimicrobial effects against bacteria, fungi and viruses and anti-inflammatory properties [16–19]. Sondi and Salopek-Sondi demonstrated that AgNPs have excellent antibacterial activity against *Escherichia coli* [19]. In the presence of 10^5 colony-forming unit

Future Medicine

(CFU) of *E. coli*, 10 μg/cm^3 of AgNPs inhibited bacterial growth by 70%. In addition to this, scanning electron microscopy (SEM) showed that the treated bacterial cells were significantly changed and presented major damage, which was characterized by the formation of 'pits' in their cell walls. Moreover, Monteiro *et al.* showed that AgNPs ranging from 0.4 to 3.3 μg/ml exhibited fungicidal activity against *C. albicans* and *C. glabrata* [12].

Despite the promising antimicrobial effects, most techniques used to synthesize these nanoparticles are expensive and may affect the environment, biological systems and human health, because they involve the use of toxic and hazardous chemicals [20]. As a solution, 'green' processes to synthetize AgNPs have been developed. This alternative utilizes biological systems, such as yeast, fungi, bacteria and plant extracts offering, thus, a comparatively safer and eco-friendly approach in relation to the chemical methods, because no-toxic substances are used. The use of plant extracts is considered a popular technique due to many reasons that include: vast and accessible reserves, large distribution, safe handling, availability of wide range of metabolites with strong reducing potentials and minimal waste and energy costs [20,21]. Extracts from plants, in particular, *Punica granatum L.* (pomegranate) have been widely used as reducing agents for Ag^+ ions [22–24]. Pomegranate is characterized by high phenolic contents – punicalagin, punicalin, ellagitannins, gallic acid, ellagic acid and anthocyanins – that exhibit favorable properties against various inflammatory disorders [25]. It is believed that the polyphenols including ellagic acid and gallic acid are the elements responsible for the reduction of Ag^+ ions and the stabilization of AgNP [26,27].

In addition to AgNPs, some calcium phosphate composites are being developed to prevent dental caries. These materials, which are similar to the mineral phase of hard tissues, can release calcium (Ca) and phosphate (P) ions to remineralize tooth lesions [28]. Several studies have demonstrated great results on enamel remineralization with polyphosphates [29–32]. Among these compounds, calcium glycerophosphate (CaGP), which is used medically as a source of Ca and P, has demonstrated anticariogenic properties [33,34].

Because of the complexity of oral biofilms and the caries development process, we predict that the association of AgNPs with CaGP can result in a promising novel biomaterial with strong antimicrobial activity and desirable remineralization properties. Thus, the aim of this study was to synthesize and characterize nanocomposites produced through a 'green' process using extracts of different parts of a *P. granatum* associated to CaGP and evaluate their antimicrobial activity against planktonic cells and biofilms of *S. mutans* and *C. albicans*.

Materials & methods

Preparation of the extracts

Extracts of the peels, leaves and seeds of pomegranate (*P. granatum L.*) were produced. Pomegranate fruits and plants were bought at a local supermarket in São Paulo (CEAGESP – Company Warehouses and General Warehouses of São Paulo). A specimen of the plant was kept in the Herbarium of the University of São Paulo, Ribeirão Preto, SP, Brazil.

Pomegranate fruits and leaves of the plants were washed with deionized water several times to remove impurities. The fruits were manually peeled and the seeds separated. Peels, leaves and seeds were dried in an incubator at 50°C, and ground into powder form using a blender [35]. The powder was then filtered through a 42-mesh sieve to obtain a standardized particle size [36].

A maceration and percolation process was employed to prepare the extracts of the different pomegranate parts [37]. For this, 30 g of each powder was macerated in 70% ethanol solution at room temperature for approximately 1 h, followed by percolation. The extracts obtained were concentrated in a rotary evaporator under reduced pressure and controlled temperature (40–60°C) [36]. After solvent evaporation, the soft extract was resolubilized to be used as the reducing agent to synthesize the nanocomposites. In order to evaluate the efficiency of the extraction process, chemical analyzes of the extracts were performed.

Chemical analyzes of the extracts

Total phenolic concentration in the extracts was measured using the Folin–Denis method as described by Singleton and Rossi [38]. Briefly, the extracts (70–95 mg) were diluted in deionized water (50 ml), homogenized and kept for 30 min in UV bath. A volume of 0.5 ml of the samples was mixed with 2.5 ml of reagent of the Folin–Denis followed by addition of 5.0 ml of 29% sodium carbonate. The samples were kept at room temperature (25°C) for 30 min. The mixture was vortexed and absorbance read at 760 nm using a UV-visible spectrophotometer (Thermo Scientific Technologies, WI, USA). Total phenolic concentration was calculated using a gallic acid (Sigma-Aldrich, Taufkirchen, Germany) standard curve and expressed as milligram gallic acid equivalent per gram.

For ellagic acid content (EAC) quantification, first, the extracts were weighed, dissolved in methanol and properly homogenized using a vortex. The samples remained for 30 min in a UV bath and, after this, they were filtered. Quantification of EAC was conducted on an HPLC (Shimadzu apparatus equipped with a communication bus module (CBM) controller, LC-20AT quaternary pump, a SPD-M 20A diode-array detector and auto sampler, Shimadzu LC solution software, version 1.21 SP1) using a 100 mm × 2.6 mm Shim pack ODS C18 column [39,40]. The wavelength was set at 254 nm and separations were carried out at a column oven temperature of 25°C. The mobile phase used for ellagic acid consisted of methanol (A) and 2% acetic acid aqueous solution, at a flow rate adjusted to 1.0 ml/min. A gradient program was applied as follows: (0–7 min, 20–72.5% A; 7–7.5 min, 72.5–95% A; 7.5–8.5 min, 95% A; 8.5–9 min, 95–20% A; 9–10 min, 20% A). The concentrations of ellagic acid were obtained using calibration curves. All assays were carried out in triplicates.

Synthesis & characterization of nanocomposites

Nanoparticles of β-CaGP were prepared at the Interdisciplinary Laboratory of Electrochemistry and Ceramics (Department of Chemistry, Federal University of São Carlos, São Carlos, SP, Brazil). 70 g of micrometric CaGP (80% β-isomer and 20% rac-α-isomer, CAS 58409-70-4, Sigma-Aldrich Chemical Co., MO, USA) was ball-milled using 500 g of zirconia spheres (diameter of 2 mm) in 1 l of isopropanol (Merck KGaA, Darmstadt, Deutschland, Germany). After 24 h, the resulting powder was separated from the alcoholic media and ground in a mortar. SEM was used to image the resulting nanoparticles of CaGP.

The 'green' synthesis of AgNPs and association with CaGP was conducted according to Gorup *et al.* [41] with some modifications. Initially, 0.042 g of silver nitrate ($AgNO_3$, Merck KGaA) was dissolved in 10 ml of deionized water heated to 90°C. Then, 0.25 g of CaGP and 0.5 ml of ammonium salt of polymethacrylic acid (Polysciences, Inc., PA, USA) were added followed by 0.07 g of aqueous extracts of *P. granatum* (peels, seeds or leaves). The reaction happened under constant agitation at 95°C for 10 min. The same process was repeated without the addition of CaGP to produce a control consisting of nanocomposites without CaGP. In total, six antimicrobial solutions were obtained: from peels extract: AgNP+CaGP (P1) and AgNP (P2); from leaves extract: AgNP+CaGP (L1) and AgNP (L2); and from seeds extract: AgNP+CaGP (S1) and AgNP (S2). During the study, all antimicrobial solutions were stored in dark bottles at 4°C.

The formation of the nanoparticles was confirmed by UV-visible spectroscopy (spectrophotometer Shimadzu MultiSpec-1501, Shimadzu Corporation, Tokyo, Japan) and, later, by x-ray diffraction (XRD; Difractometer Rigaku DMax-2000PC, Rigaku Corporation Tokyo, Japan). SEM on a Zeiss Supra 35VP microscope (S-360 microscope, Leo, MA, USA) was used in order to characterize the particles morphology. In addition, analyses by energy dispersive x-ray detector with mapping in 2D were also performed. The images were reconstructed by evaluating the energy release from the emission of some chemicals: Si Kα, O Kα, P Kα, Ag Lα1 and Ca Kα and assigning random colors to highlight silver (Ag), oxygen (O), silicon (Si), P and Ca.

In addition, the Ag^+ content of the nanocompounds was determined using a specific electrode 9616 BNWP (Thermo Scientific, MA, USA) connected to an ion analyzer (Orion 720 A^+; Orion Research, Inc., MA, USA). The combined electrode was previously calibrated with standards containing from 6.25 to 100 μg Ag^+/ml and Ag ionic strength adjuster solution (cat. no. 940011) was used (1 ml of each sample/standard: 0.02 ml ionic strength adjuster solution). The results were expressed as μg Ag^+/ml.

Antimicrobial activity

Minimum fungicidal concentration & minimum bactericidal concentration

Initially, the minimum fungicidal/bactericidal concentrations (minimum fungicidal concentration [MFC] and minimum bactericidal concentration [MBC]) were determined using the microdilution method according to the Clinical Laboratory Standards Institute (documents M27-A2 and M07-A9) [42,43] with modifications. Two reference strains from the American-Type Culture Collection (ATCC, University Boulevard, VA, USA) were used: *C. albicans* (ATCC 10231) and *S. mutans* (ATCC 25175). These microorganisms were subcultured on sabouraud dextrose agar (SDA; Difco, Le Pont-de-Claix, France) aerobically and Mueller–Hinton (MH, Difco) at 5% of CO_2, respectively, both for 24 h at 35°C. The suspensions concentrations were adjusted in 0.85% saline solution to a turbidity equivalent to 0.5 McFarland standard (1×10^6 for *C. albicans* UFC/ml and 1×10^8 for *S. mutans* UFC/ml). *S. mutans* was then diluted 20-times (5×10^6 UFC/ml) in MH supplemented with 5% of glucose while *C. albicans* was diluted 100-times (1×10^4 UFC/ml) in Roswell Park Memorial Institute medium (RPMI-1640, Sigma-Aldrich) to obtain the final inocula concentrations.

10.2217/fmb-2017-0173

Plates were set up by adding a volume of 100 µl of each compound to the first column of 96-well microtiter plates (Costar, MA, USA) containing 100 µl of RPMI for testing of *C. albicans* and 100 µl of MH with 5% glucose for testing of *S. mutans*. Sequentially, the compounds were serially diluted to a final concentration ranging from 1:2 to 1:512. Finally, 5 µl of *C. albicans* and 10 µl of *S. mutans* suspension were added to each well. The plates were incubated aerobically for 48 h for *C. albicans* and for 24 h in 5% CO_2 for *S. mutans* both at 35°C. After the incubation period, the contents of the wells were plated on SDA (for *C. albicans*) and brain heart infusion (BHI) agar (for *S. mutans*) to determine the MFC and MBC. Ellagic acid (≥96.0%, CAS 476-66-4, Sigma-Aldrich Chemical Co.) and punicalagin (≥98.0%, CAS 65995-63-3, Sigma-Aldrich Chemical Co.) also were tested, since the pomegranate peel extract presents these compounds in its composition. Three independent MFC/MBC assays were conducted for each compound/microorganism combination.

Biofilm killing

24-h-old biofilms of *C. albicans* and *S. mutans* formed in 96-well polystyrene plates (Costar) were challenged with the nanocomposites.

For the obtainment of the biofilms, *S. mutans* ATCC 25175 was subcultured on BHI agar (Difco) at 5% CO_2 and *C. albicans* ATCC 10231 was subcultured on SDA (Difco) both at 37°C for 24 h. Colonies were picked to inoculate 10 ml of BHI broth (Difco) for *S. mutans* and 10 ml of sabouraud dextrose broth (Difco) medium for *C. albicans*. After incubation at 37°C for 18 h in the presence of 5% CO_2 for *S. mutans*, cells were harvested by centrifugation (8000 rpm, 5 min), washed twice in phosphate-buffered saline (PBS; pH 7, 0.1 M) and concentrations adjusted in artificial saliva (AS) medium [12]. For *C. albicans*, we used 1×10^7 cells/ml and for *S. mutans* 1×10^8 cells/ml.

For biofilm formation, a volume of 200 µl of cell suspensions was placed into each well and incubated at 37°C in a 5% CO_2 atmosphere. After 24 h, the medium was aspirated and the wells washed with 200 µl of PBS to remove nonadherent cells before treatments.

To test killing, two antimicrobial solutions were chosen: P1 and P2. *S. mutans* biofilms were treated with 1562.0, 781.0 and 312.4 mg Ag/l of the drug P1, which represents tenfold, fivefold and twice the MBC's value, respectively. For drug P2, biofilms were treated with 781.0, 390.5, 156.2, 78.1, 39.0 and 19.5 mg Ag/l, corresponding to 10 MBC, 5 MBC, 2 MBC, MBC, $\frac{1}{2}$ MBC and $\frac{1}{4}$ MBC. *C. albicans* biofilms were treated with 1562.0 (P1) and 3125.0 (P2) mg Ag/l, which translates to tenfold the MFC's value. The antimicrobial solutions (P1 and P2) were diluted in AS medium to obtain the concentrations mentioned above. Positive control (PC) and negative control (NC) used were: chlorhexidine gluconate (CHG; Periogard, Colgate Palmolive Industrial Ltd., São Paulo, Brazil) at a concentration of 180 mg/l was used as a PC while AS medium served as an NC as the compounds were diluted in saliva.

After treatment for 24 h at 37°C in 5% CO_2, the solutions were aspirated and biofilms washed once with PBS to remove planktonic cells. Afterward, the wells containing biofilms and PBS were scraped using cell scraper. Resulting suspensions were, then, transferred to an eppendorf tubes (1.0 ml), vigorously vortexed for 1 min to disaggregate biofilm cells, serially diluted in PBS and plated on SDA and BHI agar. The plates were incubated at 37°C and after 24–48 h the total number of CFUs per unit area ($\log_{10}$ cm^{-2}) of each well was quantified.

All assays were performed independently and in triplicate.

Statistical analysis

For statistical analysis, SigmaPlot 12.0 (Systat Software, Inc., CA, USA) was used, and the significance level was set at 5%. The content of ellagic acid and phenolic compounds at the pomegranate extracts and CFU data for *C. albicans* showed normal (the Shapiro–Wilk test) and homogeneous (the Cochran test) distributions, and, one-way ANOVA was performed, followed by the Student–Newman–Keuls test. CFU data for *S. mutans* did not pass the normality test, therefore the Kruskal–Wallis test was performed followed by the Student–Newman–Keuls test.

Results

Chemical characterization of the extracts

The concentrations of ellagic acid and phenolic compounds in the peels, leaves and seeds of pomegranate are presented in Table 1. The EAC in the peel extract was statistically higher than the values for the other extracts ($p < 0.001$). However, the leaves extract presented the highest concentrations for phenolic compounds, when compared with the other extracts ($p < 0.001$). The seeds extract presented the smallest values for both ellagic acid and phenolic compounds ($p < 0.001$).

Table 1. Concentration of ellagic acid (mg/g) and phenolic compounds (mg gallic acid/g) at the pomegranate extracts.

Extracts	Ellagic acid	Polyphenols
Peels	4.2 ± 0.1[a*]	158.6 ± 4.5[b]
Leaves	2.4 ± 0.1[b]	286.5 ± 7.1[a]
Seeds	1.3 ± 0.1[c]	6.2 ± 0.1[c]

*Distinct superscript lowercase letters indicate statistical significance in each column (the Student–Newman–Keuls test, $p < 0.001$).

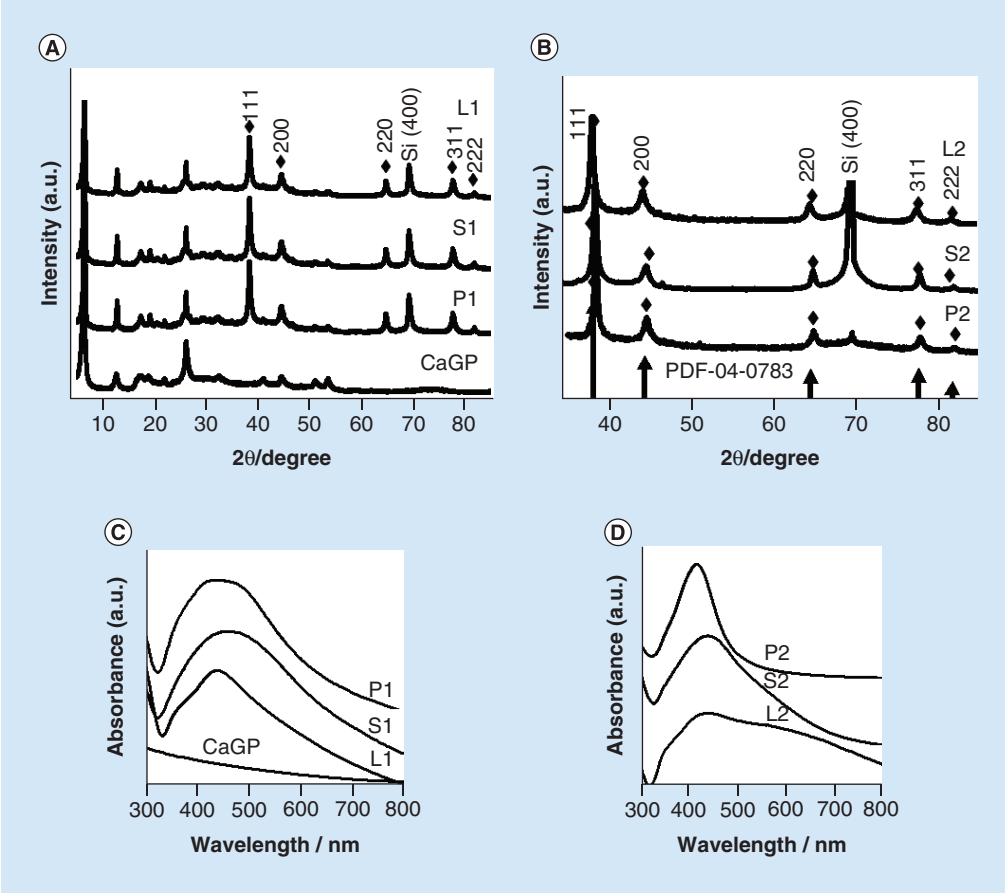

Figure 1. XRD pattern (A and B) and UV-Visible spectrum (C and D) of the nanocomposites. (A) XRD pattern of the nanocomposites P1, S1 and L1 and β-CaGP; **(B)** XRD pattern of the nanocomposites P2, S2 and L2; **(C)** UV-visible spectrum of the nanocomposites P1, S1, L1 and CaGP; **(D)** UV-visible spectrum of the nanocomposites P2, S2 and L2. CaGP: Calcium glycerophosphate; XRD: X-ray diffraction.

Structural characterization of nanocomposites

Figure 1A & B shows the diffractograms of the nanocomposites obtained by the 'green' via. The typical powder XRD pattern of the prepared CaGP showed diffraction peaks at $2\theta = 6.38°$, 12.5°, 26.4°, 41.1° and 44.3° (Figure 1A) and the corresponding crystallographic form [44]. The typical powder XRD pattern of the AgNPs showed (Figure 1B) diffraction peaks at $2\theta = 38.3°$, 44.5°, 64.7°, 77.6° and 81.7°, which can be indexed to (111), (200), (220), (311) and (222) planes of pure Ag with face-centered cubic system (PDF № 04-0783). No alteration of the crystalline structure was observed in the nanocompounds when compared with the XRD patterns of CaGP and AgNPs (PDF № 0400783).

The nanocomposites produced in this study presented chocolate brown color indicating, thus, the formation of AgNPs. The reduction of Ag^+ ions by pomegranate extracts and formation of AgNPs was also confirmed by the presence of a plasmon band between 420 and 450 nm (UV-Vis) for all the nanocomposites (Figure 1C & B).

Figure 2A–F shows SEM micrographs of the AgNPs produced with the different extracts. The NPs exhibited

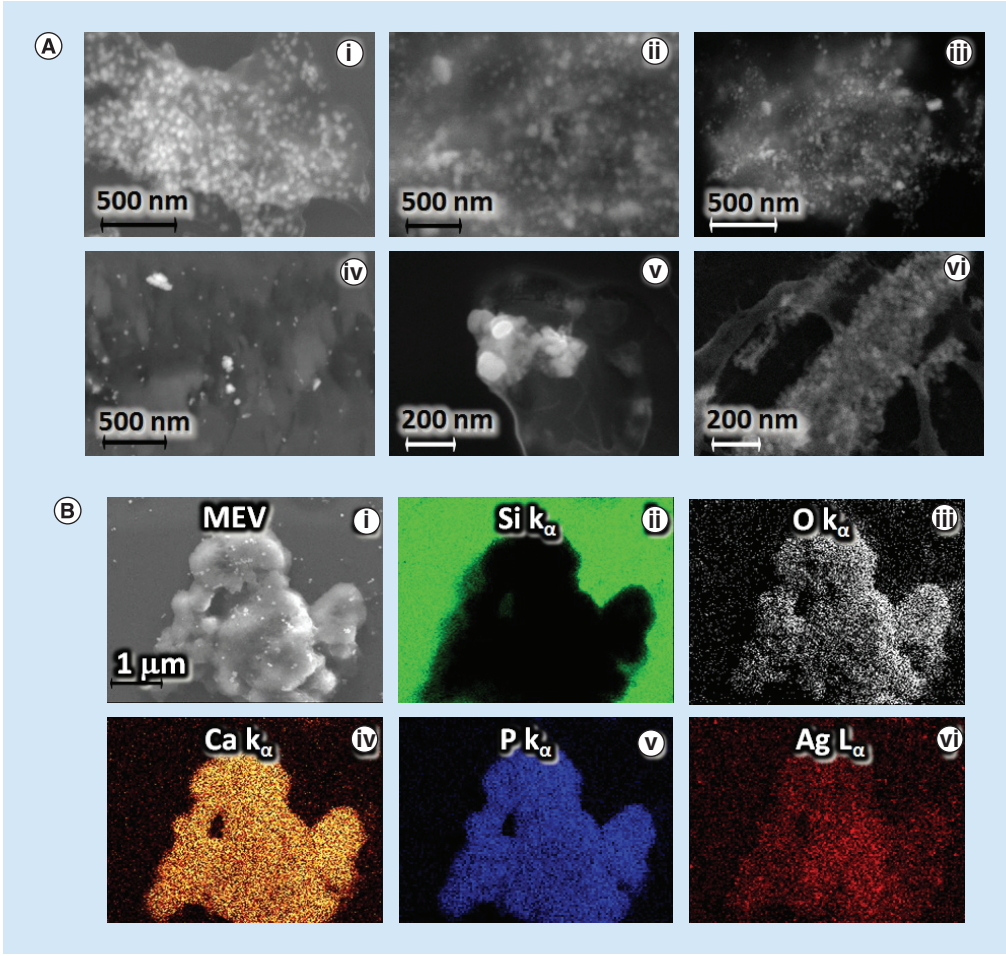

Figure 2. SEM micrographs (A) and EDS (B) of the nanocomposites. (A) SEM micrographs of nanocompounds: **(i)** P1; **(ii)** L1; **(iii)** S1; **(iv)** P2; **(v)** L2 and **(vi)** S2. **(B)** SEM and EDS mapping of the 2D elements issuance Si Kα, O Kα, Ca Kα, P Kα and Ag Kα false color. Analysis of the distribution of silver nanoparticles on the CaGP (P1 nanocompound); **(i)** SEM image; **(ii)** chemical mapping of silicon element present in the substrate, where the electron beam was focused directly on the substrate and is showed in green color, and the dark regions the beam was focused in P1 nanocomposite; **(iii–vi)** oxygen, calcium, phosphorus and silver, respectively, demonstrating that they are constituents of the P1.
EDS: Energy-dispersive x-ray spectroscopy; SEM: Scanning electron microscopy.
For color figures please see online at https://www.futuremedicine.com/doi/full/10.2217/fmb-2017-0173

spherical shape and regular distribution with size of approximately 50 nm. In the nanocompounds, P1, L1 to S1, the AgNPs were decorating the surface of the CaGP without a definite shape. Figure 2B shows the energy-dispersive x-ray detector images mapped in 2D of the compound P1 and setup by the analyzing the energy released from the issuance Si Kα, O Kα, P Kα, Ca Kα and Ag Kα, indicating the distribution of these elements on the demarcated area in the micrograph.

Ag^+ ions concentration

The results of the Ag^+ ions concentration are shown in Table 2. The nanocomposites P1, P2, S1 and S2 presented the smallest values of Ag^+ ions when compared with the compounds L1 and L2.

Antimicrobial activity

MFC & minimum bactericidal concentration

Table 3 presents the MFC and MBC of compounds against the microorganisms tested. *C. albicans* ATCC 10231 was more susceptible to the nanocomposites L1 and L2 while *S. mutans* ATCC 25175 was more susceptible

Table 2. Quantification of Ag^+ ions in the nanocomposites synthesized by the 'green' route.

Extracts	Group	Composition	μg Ag^+/ml
Peels	P1	AgNP+CaGP	0.05
	P2	AgNP	0.11
Seeds	S1	AgNP+CaGP	0.08
	S2	AgNP	0.14
Leaves	L1	AgNP+CaGP	384.7
	L2	AgNP	286.8

AgNP: Silver nanoparticle; CaGP: Calcium glycerophosphate.

Table 3. Minimum fungicidal concentration and minimum bactericidal concentration of the compounds against microorganisms tested.

Extracts	Group	Composition	MFC/MBC (mg/l)	
			C. albicans	*S. mutans*
Peels	P1	AgNP+CaGP	156.2	156.2
	P2	AgNP	312.5	78.1
Seeds	S1	AgNP+CaGP	312.5	156.2
	S2	AgNP	>1250.0	625.0
Leaves	L1	AgNP+CaGP	9.8	625.0
	L2	AgNP	4.9	1250.0
Ellagic acid			>14.5	>14.5
Punicalagin			>555.1	>555.1

AgNP: Silver nanoparticle; CaGP: Calcium glycerophosphate; MBC: Minimum bactericidal concentration; MFC: Minimum fungicidal concentration.

to the nanocomposites P1 and P2. In general, the CaGP-AgNPs presented lower MFC/MBC values than the solutions without the polyphosphate, with the exception of P1 for *S. mutans* and L1 for *C. albicans*. Ellagic acid and Punicalagin were not effective against *C. albicans* ATCC 10231 and *S. mutans* ATCC 25175.

Biofilm killing

Figure 3 shows the results of the quantification of cultivable biofilm cells. Treatment of *C. albicans* ATCC 10231 biofilms with the nanocomposites associated or not to CaGP (P1 and P2) did not result in statistically significant reduction of CFUs compared with the NC (Figure 3B). However, for *S. mutans* ATCC 25175, treatments significantly killed biofilms in a concentration-depend manner (Figure 3A). There was no statistical difference between P1 at a concentration of 312.4 mg Ag/l in comparison to the PC (CHG). Concentrations above 312.4 mg Ag/l were more effective than the CHG resulting in significant reduction of CFUs when compared with the NC ($p < 0.001$). For the P2 concentrations below 156.2 mg Ag/l were similar to CHG, while concentrations equal or higher than 156.2 mg Ag/l significantly reduced the numbers of CFUs ($p < 0.001$) even more effectively than the PC.

Discussion

In this study, we synthesized novel nanocomposites through a 'green' route with extracts of pomegranate (*P. granatum L*). Pomegranate extracts have been used to obtain a series of metallic nanoparticles, such as Ag and gold [22–23,26]. The synthesis of nanoparticles using a 'green' process is an alternative to traditional methods, with many advantages because it is an eco-friendly, clean, nontoxic and inexpensive method [14].

Plants have been used in the biosynthesis of nanoparticles as they have the capacity of producing a large variety of secondary metabolites with strong reducing potentials [20,45]. We utilized extracts of different parts of the pomegranate (peels, leaves and seeds) in order to obtain AgNPs since these extracts presented high concentrations of phenolic compounds, including ellagic acid and gallic acid, known for their antimicrobial properties [46]. These compounds are, probably, the elements responsible for the reduction of Ag^+ ions and the stabilization of AgNP [26,27]. The addition of CaGP to produce AgNP-CaGPs did not interfere with the reduction process of the

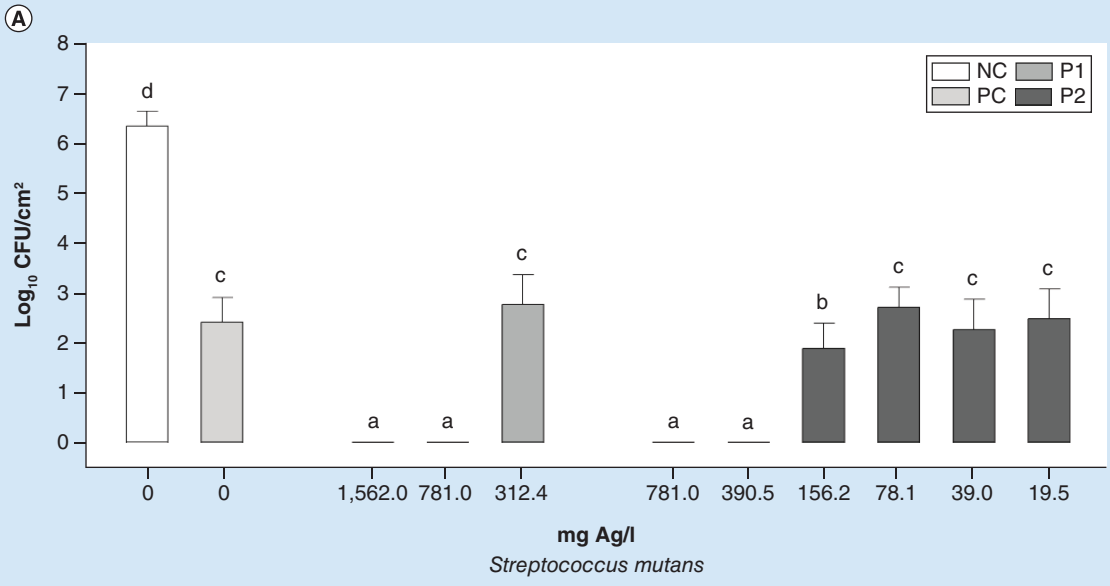

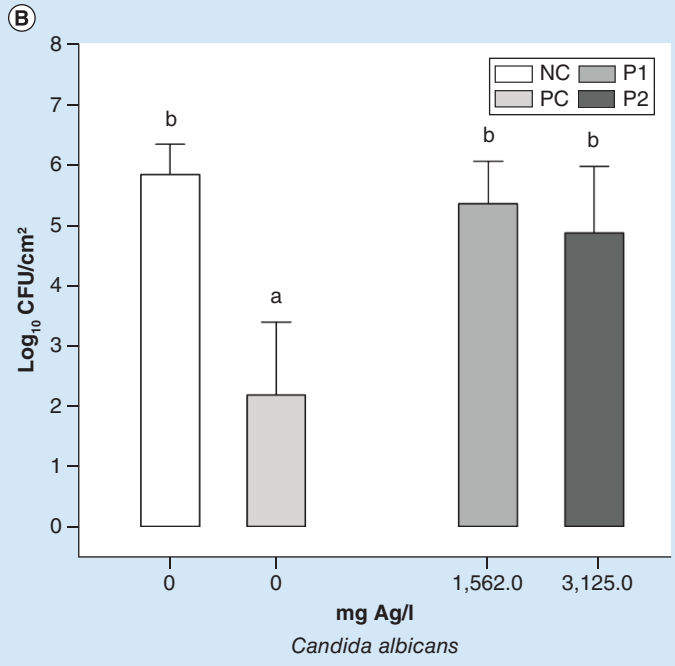

Figure 3. Mean values (±SD) of biofilm cells after treatment expressed as log_{10} CFU/cm^2 for *S. mutans* (A) and *C. albicans* (B) single biofilms. NC (saliva); PC = Chlorhexidine gluconate (180 mg/l); P1 = AgNP+CaGP; P2 = AgNP. Different lowercase letters indicate significant difference among the treatments for *S. mutans* ($p < 0.05$; the Kruskall–Wallis test) and *C. albicans* biofilms ($p < 0.05$; the Student–Newman–Keuls test).
AgNP: Silver nanoparticle; CaGP: Calcium glycerophosphate; NC: Negative control; PC: Positive control; SD: Standard deviation.

Ag^+ ions. Sodagar *et al.* also synthesized a novel compound containing AgNPs and hydroxyapatite and similarly did not observe interference of the calcium compound in the production of the nanoparticles [47].

The first qualitative indication of nanoparticle synthesis is the color change of the reaction solution from yellow to brown due to surface plasmon vibration [48]. In our study, all nanocompounds had an immediate change in color, becoming chocolate brown. In addition, the quantification of Ag^+ ions in the compounds solutions showed a reduced presence of Ag^+ ions compared with the presynthesis mixture measurements indicating the conversion of Ag^+ ions into nanoparticles. The reduction of Ag^+ ions by pomegranate extracts was also confirmed by the presence

of a plasmon band (UV-Vis) between 420 and 450 nm for all composites, evidencing the formation of AgNPs [48]. The antioxidant activity of pomegranate extracts might be responsible for the reduction of the Ag^+ ions, since plant extracts contain phytochemicals (ellagic acid, gallic acid and punicalagin) and secondary metabolites [48] that lead to formation of H^+ radicals, which reduce the size of Ag to nanosize [22].

Calcium phosphate composites have been developed to release calcium and phosphate ions to remineralize tooth lesions because of their demonstrated anticariogenic properties [30,34,49–52]. In fact, Hannig and Hannig reported the successful remineralization of incipient enamel lesions with AgNPs combined with hydroxyapatite [53]. Therefore, one of the goals of this study was to combine the potential remineralization benefits of CaGP to the microbial-killing effects of nanoparticles. The novel composites obtained through the 'green' route here presented possess antimicrobial activity against *S. mutans* and *C. albicans*. Some solutions, namely, L1 and L2, were more effective against *C. albicans*, which can be explained by the higher concentration of Ag^+ ions present in these compounds in comparison to the others where a greater conversion of Ag^+ ions to nanoparticles was achieved. The literature reports that ionic Ag presents notable antimicrobial activity [54,55] despite the associated cytotoxicity [56,57].

Although the antimicrobial mode of action of nanoparticles is not completely understood it has been suggested that the interaction of Ag with thiol groups of proteins on the cell wall increases the membrane permeability leading to pore formation and thereby causing bacterial death [58–61]. On the other hand, activity against *S. mutans* required a higher concentration of AgNPs in these compounds (L1 and L2). Probably, this fact is related with particle size. The compounds L1 and L2 presented larger particles in relation to the other compounds. The literature reveals that smaller particles penetrate more easily through cell membrane, interacting with intracellular materials and finally resulting in cell destruction in the process of multiplication [48]. Some authors also have reported that Gram-negative bacteria are more susceptible to AgNPs compared with Gram-positive bacteria [48], because Gram-positive bacteria possess a 3D peptidoglycan layer of approximately 80 nm (ten-times thicker than Gram-negative bacteria) [62–65].

Microorganisms can form structured, coordinated and functional communities consisted of adherent cells (sessile cells) called biofilms that pose a major clinical concern due to antimicrobial tolerance. Many antimicrobial agents, who are effective against free-living planktonic bacterial cells, are ineffective against the same species growing in a biofilm state. This has motivated the scientific community to search for agents capable of eradicating these resistant bacterial phenotypes. The challenge is extended to developing formulations suitable for oral use and efficient not only against microorganisms causing dental caries and denture stomatitis [65] but also capable of preventing and reverting enamel demineralization. In this study, a model of biofilm formation on the wells of microtiter plates was used in order to evaluate the antimicrobial effects of selected AgNPs associated or not to CaGP against *S. mutans*- and *C. albicans*-preformed biofilms. The pomegranate was just utilized to produce AgNPs and the phenolic compounds present in the pomegranate (ellagic acid and punicalagin) were previously tested and did not present antimicrobial effect. The nanocomposites P1 and P2 were chosen to be tested against biofilms because presented low MFC (for *C. albicans*) and MBC (for *S. mutans*) values. These nanocomposites were effective against *S. mutans* 24-h biofilms with results similar or even better than chlorhexidine, which is the gold standard in terms of oral antiseptics. Furthermore, our results indicated that there was a dose-dependent inhibitory effect both for P1 and P2. It can be also observed that the presence of CaGP reduced the effect of the nanoparticles. It might have occurred because AgNPs were decorating the surface of the glycerophosphate and, therefore, were are not completely available. However, a pilot study conducted by our research group showed that the concentration of 312.4 mg Ag/l (that reduced the CFU similarly to chlorhexidine) of the antimicrobial solution P1 was not toxic to odontoblastic cells [Botazzo Delbem AC, Barbosa DB Unpublished Data]. One hypothesis to explain the effect of AgNPs against *S. mutans* is their interaction with the bacterial cell membrane. It induces formation of pores in the membrane, with consequent internalization of NPs, and then causes further damage to the cells due to their interaction with both intracellular proteins and DNA affecting the cell's ability to replicate [66,67]. Another hypothesis of how the nanoparticles affect the cells is that they the release active Ag ions that interact with proteins and receptors in the cell membranes [67].

AgNPs have shown efficacy against *C. albicans* [68,69], by disturbing the membrane and creating pores; provoking, thus, cellular apoptosis [70]. Interestingly, in our study, composites P1 and P2 were not effective against *C. albicans*-preformed biofilms (Figure 2). Biofilms are enclosed in a self-produced protective extracellular matrix that can hamper the penetration of the AgNPs. Lara *et al.* demonstrated that this matrix may contribute to the reduced susceptibility of preformed biofilms to AgNPs [70]. Another factor that can explain its resistance to NPs is the presence of persister cells. This mechanism is observed in chronic infections [71] and, recently, has gathered special attention in fungal biofilms [72]. Persister cells are 'dormant variants' of regular cells that form in microbial populations and

are able to survive even in the presence of antibiotics well above the MIC [73,74]. Moreover, *C. albicans* presents a cell wall besides a cellular membrane. The cell wall is essential to nearly every aspect of the biology and pathogenicity of fungi, with pivotal functions in adhesion properties and morphogenetic conversions and it is composed mostly of glucans, chitin and mannoproteins [75]. These characteristics may hinder the effect of AgNPs.

Conclusion

Here, we described the successful synthesis of novel AgNPs associate to CaGP using a 'green' process with pomegranate extracts. In conclusion, the compounds possess antimicrobial and antibiofilm activity against important microorganisms causing caries and candidiasis, and may be a promising novel biomaterial in dental applications. Additional studies are necessary to evaluate their effect against mixed biofilms, ability to remineralize enamel and cytotoxicity.

Future perspective

This study shows that it is possible to obtain a promising novel biomaterial with strong antimicrobial activity (AgNPs) and desirable remineralization properties (calcium phosphate – β-CaGP). Moreover, we utilized a 'green' synthesis (different extracts of pomegranate were utilized) that is a comparatively safer and eco-friendly approach in relation to other techniques that involve the use of toxic and hazardous chemicals. Oral bacteria and *Candida* species have been reported in many studies that are resistant to antimicrobial agents. Thus, studies with AgNPs synthesized through a 'green' via and oral clinical isolates are being planned by our research group.

Summary points

- One of the main etiological agents in caries is *Streptococcus mutans*, a Gram-positive, facultative anaerobic, coccus-shaped bacterium, which is able to ferment several sugars, including sucrose, glucose, dextrose and lactose, producing lactic acid.
- But recently, studies have demonstrated a significant association between *S. mutans* and *Candida albicans* and early childhood caries.
- Controlling oral biofilm formation is not an easy task but in recent years, nanotherapeutics have been used with success by incorporating nanoparticles into several dental materials.
- Because of the complexity of oral biofilms and the caries development process, we believe that the association of silver nanoparticles (AgNPs) with β-calcium glycerophosphate (CaGP) can result in a promising novel biomaterial with strong antimicrobial activity and desirable remineralization properties.
- Thus, we synthesized nanocomposites (AgNP-CaGP) through a 'green' route with different extracts of pomegranate.
- Compounds possess antimicrobial/antibiofilm activity against *S. mutans* and *C. albicans*.
- Composites made with peel extracts showed similarly or even better than chlorhexidine.
- The association AgNP-CaGP may be a promising biomaterial in dental applications. However, additional studies are necessary to evaluate their effect against mixed biofilms, ability to remineralize enamel and cytotoxicity.

Financial & competing interests disclosure

This work was supported by CAPES Foundation, Ministry of Education of Brazil (processes 88881.030445/2013-01 and 88887.068358/2014-00) and the São Paulo Research Foundation (FAPESP, process 2015/00825-5). The authors have no other relevant affiliations or financial involvement with any organization or entity with a financial interest in or financial conflict with the subject matter or materials discussed in the manuscript apart from those disclosed.

No writing assistance was utilized in the production of this manuscript.

References

Papers of special note have been highlighted as: • of interest; •• of considerable interest

1. Kuboniwa M, Tribble GD, Hendrickson EL, Amano A, Lamont RJ, Hackett M. Insights into the virulence of oral biofilms: discoveries from proteomics. *Expert Rev. Proteomics* 9(3), 311–323 (2012).
2. Jakubovics NS, Kolenbrander PE. The road to ruin: the formation of disease-associated oral biofilms. *Oral Dis.* 16(8), 729–739 (2010).
3. Senneby A, Davies JR, Svensäter G, Neilands J. Acid tolerance properties of dental biofilms in vivo. *BMC Microbiol.* 17(1), 165 (2017).

4. Krzyściak W, Jurczak A, Kościelniak D, Bystrowska B, Skalniak A. The virulence of *Streptococcus mutans* and the ability to form biofilms. *Eur. J. Clin. Microbiol. Infect. Dis.* 33(4), 499–515 (2014).
5. Shimada A, Noda M, Matoba Y, Kumagai T, Kozai K, Sugiyama M. Oral lactic acid bacteria related to the occurrence and/or progression of dental caries in Japanese preschool children. *Biosci. Microbiota Food Health* 34(2), 29–36 (2015).
6. Willems HM, Kos K, Jabra-Risk MA, Krom BP. Candida albicans in oral biofilms could prevent caries. *Pathog. Dis.* 74(5), pii:ftw039 (2016).
7. Fragkou S, Balasouli O, Tsuzukibashi A *et al. Streptococcus mutans*, *Streptococcus sobrinus* and *Candida albicans* in oral samples from caries-free and caries-active children. *Eur. Arch. Paediatric. Dent.* 17(5), 367–375 (2016).

•• **Describes the occurrence of *Streptococcus mutans*, *S. sobrinus* and *Candida albicans* in dental plaque of caries-active children.**

8. Metwalli KH, Khan SA, Kromp BP, Jabra-Rizk MA. *Streptococcus mutans*, *Candida albicans*, and the human mouth: a sticky situation. *PLoS Pathog.* 9(10), e1003616 (2013).
9. Klinke T, Guggenheim B, Klimm W, Thurnheer T. Dental caries in rats associated with *Candida albicans*. *Caries Res.* 45(2), 100–106 (2011).
10. Gregoire S, Xiao J, Silva BB *et al.* Role of glucosyltransferase B in interactions of *Candida albicans* with *Streptococcus mutans* and with an experimental pellicle on hydroxyapatite surfaces. *Appl. Environ. Microbiol.* 77(18), 6357–6367 (2011).
11. Noronha VT, Paula AJ, Durán G *et al.* Silver nanoparticles in dentistry. *Dent. Mater.* 33(10), 1110–1126 (2017).
12. Monteiro DR, Gorup LF, Silva S *et al.* Silver coloidal nanoparticles: antifungal effect against adhered cells and biofilms of *Candida albicans* and *Candida glabrata*. *Biofouling* 27(7), 711–719 (2011).

• **Describes the effect of silver nanoparticles (AgNPs) against *C. albicans*-adhered cells and biofilms.**

13. Jahromi MAM, Zangabad PS, Basri SMM *et al.* Nanomedicine and advanced technologies for burns: preventing infection and facilitating wound healing. *Adv. Drug Deliv. Rev.* 123, 33–64 (2017).
14. Krishna IM, Reddy GB, Veerabhadram G, Madhusudhan A. Eco-friendly green synthesis of silver nanoparticles using salmalia malabarica: synthesis, characterization, antimicrobial and catalytic activity studies. *Appl. Nanosci.* 6(5), 681–689 (2016).
15. Kushwaha A, Singh VK, Bhartariya J, Singh P, Yasmeen K. Isolation and identification of *E. coli* bacteria for the synthesis of silver nanoparticles: characterization of the particles and study of antibacterial activity. *Eur. J. Exp. Biol.* 5(1), 65–70 (2015).
16. Beyth N, Haddad YH, Domb A, Khan W, Hazan R. Alternative antimicrobial approach: nano-antimicrobial materials. *Evid. Based Complement. Alternat. Med.* 2015, 246012 (2015).
17. Nam G, Rangasamy S, Purushothaman B, Song JM. The application of bactericidal silver nanoparticles in wound treatment. *Nanomater. Nanotechnol.* 1, 5–23 (2015).
18. Tran HV, Tran LD, Ba CT *et al.* Synthesis, characterization, antibacterial and antiproliferative activities of monodisperse chitosan-based silver nanoparticles. *Colloids Surf. A: Physicochem. Eng. Aspects.* 360, 32–40 (2010).
19. Sondi I, Salopek-Sondi B. Silver nanoparticles as antimicrobial agent: a case study on *E. coli* as a model for Gram-negative bacteria. *J. Colloid. Interface Sci.* 275(1), 177–182 (2004).
20. Ali M, Kim B, Belfield KD, Norman D, Brennan M, Ali GS. Green synthesis and characterization of silver nanoparticles using *Artemisia absinthium* aqueous extract – a comprehensive study. *Mater. Sci. Eng. C Mater. Biol. Appl.* 58, 359–365 (2016).
21. Roy N, Gaur A, Jain A, Bhattacharya S, Rani V. Green synthesis of silver nanoparticles: an approach to overcome toxicity. *Environ. Toxicol. Pharmacol.* 36(3), 807–812 (2013).
22. Ahmad N, Sharma S, Rai R. Rapid green synthesis of silver and gold nanoparticles using peels of *Punica granatum*. *Adv. Mat. Lett.* 3, 376–380 (2012).

•• **Describes a simple and eco-friendly biosynthesis of silver nanoparticles (AgNPs) using pomegranate peel extracts as the reducing agent.**

23. Gnanajobitha G, Rajeshkumar S, Annadurai G, Kannan C. Preparation and characterization of fruit-mediated silver nanoparticles using pomegranate extract and assessment of its antimicrobial activities. *J. Environ. Nanotechnol.* 2(1), 4–10 (2013).
24. Nadagouda MN, Iyanna N, Lalley J *et al.* Synthesis of silver and gold nanoparticles using antioxidants from blackberry, blueberry, pomegranate and turmeric extracts. *ACS Sustainable Chem. Eng.* 2(7), 1717–1723 (2014).
25. Shaygannia E, Bahmani M, Zamanzad B, Rafieian-Kopaei M. A review study on *Punica granatum L. J. Evid. Based Complementary Altern. Med.* 21(3), 221–227 (2016).
26. Edison TJI, Sethuraman MG. Biogenic robust synthesis of silver nanoparticles using *Punica granatum* peel and its application as a green catalyst for the reduction of an anthropogenic pollutant 4-nitrophenol. *Spectrochim. Acta A Mol. Biomol. Spectrosc.* 104, 262–264 (2013).
27. Kumari A, Guliani A, Singla R, Yadav R, Yadav SK. Silver nanoparticles synthesized using plant extracts show strong antibacterial activity. *IET Nanobiotechnol.* 9(3), 142–152 (2015).
28. Xie X, Wang L, Xing D *et al.* Protein-repellent and antibacterial functions of a calcium phosphate rechargeable nanocomposite. *J. Dent.* 52, 15–22 (2016).

29. Amaral JG, Freire IR, Valle-Neto EF, Cunha RF, Martinhon CC, Delbem AC. Longitudinal evaluation of fluoride levels in nails of 18–30-month-old children that were using toothpastes with 500 and 1,100 μg F/g. *Community Dent. Oral Epidemiol.* 42(5), 412–419 (2014).
30. Zaze AC, Dias AP, Amaral JG, Miyasaki ML, Sassaki KT, Delbem AC. In situ evaluation of low-fluoride toothpastes associated to calcium glycerophosphate on enamel remineralization. *J. Dent.* 42(12), 1621–1625 (2014).
31. Dalpasquale G, Delbem ACB, Pessan JP *et al.* Effect of the addition of nano-sized sodium hexametaphosphate to fluoride toothpastes on tooth demineralization: an in vitro study. *Clin. Oral Investig.* 21(5), 1821–1827 (2017).
32. Danelon M, Pessan JP, Souza-Neto FN, de Camargo ER, Delbem AC. Effect of fluoride toothpaste with nano-sized trimetaphosphate on enamel demineralization: an in vitro study. *Arch. Oral Biol.* 78, 82–87 (2017).
33. Nagata ME, Delbem AC, Hall KB, Buzalaf MA, Pessan JP. Fluoride and calcium concentrations in the biofilm fluid after use of fluoridated dentifrices supplemented with polyphosphate salts. *Clin. Oral Investig.* 21(3), 831–837 (2017).
34. Freire IR, Pessan JP, Amaral JG, Martinhon CC, Cunha RF, Delbem AC. Anticaries effect of low-fluoride dentifrices with phosphates in children: a randomized, controlled trial. *J. Dent.* 50, 37–42 (2016).

• **Reports that calcium glycerophosphate has anticariogenic properties.**

35. Fawole OA, Makunga NP, Opara UL. Antibacterial, antioxidant and tyrosinase-inhibition activities of pomegranate fruit peel methanolic extract. *BMC Complement. Altern. Med.* 12, 200 (2012).
36. Rocha BA, Bueno PC, Vaz MM *et al.* Evaluation of a propolis water extract using a reliable RP-HPLC methodology and in vitro and in vivo efficacy and safety characterization. *Evid. Based Complement. Alternat. Med.* 2013, 670451 (2013).
37. Abreu Miranda M, Lemos M, Alves Cowart K *et al.* Gastroprotective activity of the hydroethanolic extract and isolated compounds from the leaves of Solanum cernuum Vell. *J. Ethnopharmacol.* 172, 421–429 (2015).
38. Singleton VL, Rossi JA. Colorimetry of total phenolics with phosphomolybdic-phosphotungstic acid reagents. *Am. J. Enol. Vitic.* 16, 144–158 (1965).
39. Masci A, Coccia A, Lendaro E, Mosca L, Paolicelli P, Cesa S. Evaluation of different extraction methods from pomegranate whole fruit or peels and the antioxidante and antiproliferative activity of the polyphenolic fraction. *Food Chem.* 202, 59–69 (2016).
40. Ferreira MR, Fernandes MT da Silva WA *et al.* Chromatographic and spectrophotometric analysis of phenolic compounds from fruits of *Libidibia ferrea* Martius. *Pharmacoqn. Mag.* 12(2), 285–291 (2016).
41. Gorup LF, Longo E, Leite ER, Camargo ER. Moderating effect of ammonia on particle growth and stability of quasi-monodisperse silver nanoparticles synthesized by the Turkevich method. *J. Colloid. Interface Sci.* 360(2), 355–258 (2011).
42. National Committee for Clinical Laboratory Standards. *Reference Method for Broth Dilution Antifungal Susceptibility Testing of Yeasts (2nd Edition).* NCCLS, Wayne, PA, USA (2002).
43. National Committee for Clinical Laboratory Standards. *Methods for Dilution Antimicrobial Susceptibility Tests for Bacteria That Grow Aerobically (9th Edition) – Approved Standard M07-A9*. National Committee for Clinical Laboratory Standards, Wayne, PA, USA (2012).
44. Hanawalt JD, Rinn HW, Frevel LK. Chemical analysis by x-ray diffraction classification and use of x-ray diffraction patterns. *Anal. Chem.* 10(9), 457–512 (1938).
45. Mittal AK, Bhaumik J, Kumar S, Banerjee UC. Biosynthesis of silver nanoparticles: elucidation of prospective mechanism and therapeutic potential. *J. Colloid. Interface Sci.* 415, 39–47 (2014).
46. Rosas-Burgos EC, Burgos-Hernández A, Noguera-Artiaga L *et al.* Antimicrobial activity of pomegranate peel extracts as affected by cultivar. *J. Sci. Food Agric.* 97(3), 802–810 (2017).
47. Sodagar A, Akhavan A, Hashemi E *et al.* Evaluation of the antibacterial activity of a conventional orthodontic composite containing silver/hydroxyapatite nanoparticles. *Prog. Orthod.* 17(1), 40 (2016).

• **Describes the antimicrobial properties of a new composite containing silver/hydroxyapatite nanoparticles.**

48. Patil MP, Kim GD. Eco-friendly approach for nanoparticles synthesis and mechanism behind antibacterial activity of silver and anticancer activity of gold nanoparticles. *Appl. Microbiol. Biotechnol.* 101(1), 79–92 (2017).

•• **Covers general information about the eco-friendly process for the synthesis of AgNPs and focuses on the mechanism of the antibacterial activity of AgNPs.**

49. Weir MD, Ruan J, Zhang N *et al.* Effect of calcium phosphate nanocomposite on in vitro remineralization of human dentin lesion. *Dent. Mater.* 33(9), 1033–1044 (2017).

• **Investigates the remineralization of human dentin lesions *in vitro* via restorations using nanocomposites containing calcium phosphate.**

50. Weir MD, Chow LC, Xu HH. Remineralization of demineralizaed enamel via calcium phosphate nanocomposite. *J. Dent. Res.* 91(10), 979–984 (2012).
51. Melo MA, Weir MD, Rodrigues LK, Xu HH. Novel calcium phosphate nanocomposite with caries inhibition in a human in situ model. *Dent. Mater.* 29(2), 231–240 (2013).

52. do Amaral JG, Sassaki KT, Martinhon CC, Delbem AC. Effect of low-fluoride dentifrices supplemented with calcium glycerophosphate on enamel demineralization in situ. *Am. J. Dent.* 26(2), 75–80 (2013).
53. Hannig C, Hannig M. Natural enamel wear – a physiological source of hydroxyapatite nanoparticles for biofilm management and tooth repair? *Med. Hypotheses.* 74, 670–672 (2010).
54. Morrill K, May K, Leek D *et al.* Spectrum of antimicrobial activity associated with ionic colloidal silver. *J. Alter. Complement. Med.* 19(3), 224–231 (2013).
55. Belluco S, Losasso C, Patuzzi I *et al.* Silver as antimicrobial toward *Listeria monocytogenes*. *Front. Microbiol.* 7, 307 (2016).
56. Vrček IV, Žuntar I, Petlevski R *et al.* Comparison of in vitro toxicity of silver ions and silver nanoparticles on human hepatoma cells. *Environ. Toxicol.* 31(6), 679–692 (2016).
57. Galandáková A, Franková J, Ambrožová N *et al.* Effects of silver nanoparticles on human dermal fibroblasts and epidermal keratinocytes. *Hum. Exp. Toxicol.* 35(9), 946–957 (2016).
58. Durán N, Durán M, de Jesus MB, Seabra AB, Fávaro WJ, Nakazato G. Silver nanoparticles: a new view on mechanistic aspects on antimicrobial activity. *Nanomedicine* 12(3), 789–799 (2016).
59. Pietrzak K, Glińska S, Gapińska M *et al.* Silver nanoparticles: a mechanism of action on moulds. *Metallomics* 8(12), 1294–1302 (2016).
60. Durán N, Marcato PD, de Conti R, Alves OL, Costa FTM, Brocchi M. Potential use of silver nanoparticles on pathogenic bacteria, their toxicity and possible mechanisms of action. *J. Braz. Chem. Soc.* 21, 949–959 (2010).
61. Kaviya S, Santhanalakshmi J, Viswanathan B. Green synthesis of silver nanoparticles using *Polyalthia longifolia* leaf extract along with D-sorbitol: study of antibacterial activity. *J. Nanotechnol.* 2011, 152970 (2011).
62. Chaloupka K, Malam Y, Seifalian AM. Nanosilver as a new generation of nanoproduct in biomedical applications. *Trends Biotechnol.* 28(11), 580–588 (2010).
63. Gurunathan S, Hanm JW, Kwon DN, Kim JH. Enhanced antibacterial and antibiofilm activities of silver nanoparticles against Gram-negative and Gram-positive bacteria. *Nanoscale Res. Lett.* 9(1), 373 (2014).
64. Hungund BS, Dhulappanavar GR, Ayachit NH. Comparative evaluation of antibacterial activity of silver nanoparticles biosynthesized using fruit juices. *J. Nanomed. Nanotechnol.* 6, 271 (2015).
65. Choudhary MK, Kataria J, Cameotra SS, Singh J. A facile biomimetic preparation of highly stabilized silver nanoparticles derived from seed extract of Vigna radiata and evaluation of their antibacterial activity. *Appl. Nanosci.* 6, 105–111 (2016).
66. Rizzello L, Pompa PP. Nanosilver-based antibacterial drugs and devices: mechanisms, methodological drawbacks, and guidelines. *Chem. Soc. Rev.* 43(5), 1501–1518 (2014).

• **Describes the bactericidal effects of AgNPs.**

67. Magalhães AP, Moreira FC, Alves DR *et al.* Silver nanoparticles in resin luting cements: antibacterial and physiochemical properties. *J. Clin. Exp. Dent.* 8(4), e415–e422 (2016).
68. Monteiro DR, Takamiya AS, Feresin LP *et al.* Susceptibility of *Candida albicans* and *Candida glabrata* biofilms to silver nanoparticles in intermediate and mature development phases. *J. Prosthodont. Res.* 59(1), 42–48 (2015).
69. Selvaraj M, Pandurangan P, Ramasami N *et al.* Highly potential antifungal activity of quantum-sized silver nanoparticles against *Candida albicans*. *Appl. Biochem. Biotechnol.* 173(1), 55–66 (2014).
70. Lara HH, Romero-Urbina DG, Pierce C, Lopez-Ribot JL, Arellano-Jiménez MJ, Jose-Yacaman M. Effect of silver nanoparticles on *Candida albicans* biofilms: an ultrastructural study. *J. Nanobiotechnol.* 13, 91 (2015).
71. Fauvart M, De Groote VN, Michels J. Role of persister cells in chronic infections: clinical relevance and perspectives on anti-persister therapies. *J. Med. Microbiol.* 60(Pt 6), 699–709 (2011).
72. De Brucker K, De Cremer K, Cammue BP, Thevissen K. Protocol for determination of the persister subpopulation in Candida albicans biofilms. *Methods Mol. Biol.* 1333, 67–72 (2016).
73. Lewis K. Persister cells: molecular mechanisms related to antibiotic tolerance. *Handb. Exp. Pharmacol.* 211, 121–133 (2012).
74. Fisher RA, Gollan B, Helaine S. Persistent bacterial infections and persister cells. *Nat. Rev. Microbiol.* 15(8), 453–464 (2017).
75. Free SJ. Fungal cell wall organization and biosynthesis. *Adv. Genet.* 81, 33–82 (2013).
76. Arias LS, Delbem AC, Fernandes RA, Barbosa DB, Monteiro DR. Activity of tyrosol against single and mixed-species oral biofilms. *J. Appl. Microbiol.* 120(5), 1240–1249 (2016).